MA . 530 . 135 . 1

الجمهورية الجزائرية الديمقراطية الشعبية
PEOPLE'S DEMOCRATIC REPUBLIC OF ALGERIA
وزارة التعليم العالي والبحث العلمي
MINISTERY OF HIGH EDUCATION AND SCIENTIFIC RESEARCH

جامعة سعد دحلب البليدة 1
UNIVERSITY of SAAD DAHLEB BLIDA 1
كلية العلوم – دائرة الفيزياء
Faculty of Sciences - Department of Physics

MASTER DIPLOMA THESIS

In Physics
Option: NanoPhysics.

THEME

OPTOELECTRIC PROPERTIES OF GaInP p-i-n SOLAR CELLS WITH DIFFERENT i-LAYER THICKNESSES

By:

- **NEDJARI Meriem**
- **BIRKANE Meriem**

MA-530-135-1

Members of Jury:

Mr. A. Benhaffaf	MAA Université Blida 1	President
Dr. N. Belgroune	MAB Université Blida 1	Examiner
Dr. A. Hassein-Bey	MCB Université Blida 1	Thesis Advisors.
Mr. A. Tahraoui	MAA Université Blida 1	Thesis CoAdvisors

Blida, October 2018

Abstract

The optoelectric properties of GaInP p-i-n solar cells with different intrinsic layer (i-layer) thicknesses from 0.25 to 1 μm werestudied. Both emission intensity and full width at half maximum features of the photoluminescence spectrum indicate that the optimum i-layer thickness would be between 0.5 and 0.75 μm. The integrated current results of photocurrent experiment also point out that the samples with 0.5 to 0.75 μm i-layer thicknesses have optimum value around 156 nA. Electroreflectance measurements reveal that the built-in electric field strength of the sample gradually deviates fromthe theoretical value largerwhen i-layer thickness of the sample is thicker than0.75 μm. I-Vmeasurements also confirmcrystal quality forwhole samples by obtaining the information about short currents of photovoltaic performances. A series of experiments reflect that thicker i-layer structure would induce more defects generation lowering crystal quality.

Résumé

Les propriétés optoélectriques de cellules solaires GaInP p-i-n avec différentes épaisseurs de couche intrinsèque (couche i) de 0,25 à 1 µm ont été étudiées. Les caractéristiques d'intensité d'émission et de largeur totale à mi-hauteur du spectre de photoluminescence indiquent que l'épaisseur optimale de la couche i serait comprise entre 0,5 et 0,75 µm. Les résultats actuels intégrés à l'expérience de photocourant indiquent également que les échantillons d'une épaisseur de couche i comprise entre 0,5 et 0,75 µm ont une valeur optimale autour de 156 nA. Les mesures d'électroréflectance révèlent que l'intensité du champ électrique intégré à l'échantillon s'écarte progressivement de la valeur théorique lorsque l'épaisseur de la couche i de l'échantillon est supérieure à 0,75 µm. Les mesures I-V confirment également la qualité des cristaux pour tous les échantillons en obtenant des informations sur les courants courts des performances photovoltaïques. Une série d'expériences montre que la structure plus épaisse de la couche i induirait davantage de génération de défauts réduisant la qualité des cristaux.

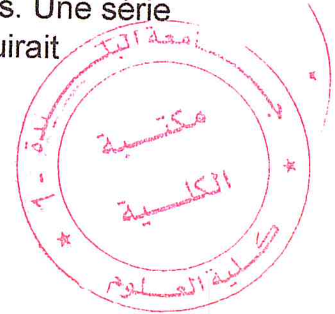

ملخص

الخصائص الكهروضوئية للخلايا الشمسية GaInP p-i-n ذات سماكة الطبقة الداخلية المختلفة (i-layer) من 0.25 إلى 1 ميكرومتر. تشير كل من كثافة الانبعاث والعرض الكامل عند نصف خصائص الحد الأقصى لطيف الضوء الضوئي إلى أن سمك الطبقة i الأمثل سيكون بين 0.5 و 0.75 ميكرومتر. تشير النتائج الحالية المتكاملة للتجربة الضوئية إلى أن العينات ذات سماكة الطبقة i إلى 0.55 μm havem لها القيمة المثلى حول 156 nA. تكشف قياسات الانعكاس الكهربائي أن شدة المجال الكهربائي الداخلي للعينة تنحرف تدريجياً عن القيمة النظرية الأكبر عندما تكون سماكة الطبقة i في العينة أكثر سمكا من 0.75 ميكرومتر. I-Vmeasurements أيضا التأكد من جودة ثقوب العينات من خلال الحصول على معلومات حول تيارات قصيرة من الأداء الضوئية. وتعكس سلسلة من التجارب أن البنية السميكة للطبقة i من شأنها أن تحفز المزيد من العيوب على خفض جودة البلورا

Acknowledgements

First and formost, we would like to thank ALLAH all mighty for givin us the grace and strength till this very day of our master program, we also would like to thank the two persons that Allah has blessed us with in our life; ***Our Parents*** who sacrificed their youth and energy, and gave us all their love and support to transform the lives they gave us into wonderful adventures. We are so glad and blessed to be able to wake up every day and see their smiles. We wish that we make them proud, and that they can finally pick up the fruits of their efforts.

Secondly, we would be more than glad to thank our advisor "Dr. Ahmed Tahraoui" for all the patience, time and efforts that he was so generous to give to us during the period of accomplishing this work. Despite him being very far from his homeland, which caused some difficulties in communication, and the fact that we knew very little about Solar Energy did not prevent him from believing in us and giving us opportunity to learn and work with him. This allowed us to gain valuable knowledge, experience, confidence and a strong will to accomplish this work and try to contribute to the field of Solar Energy. We wish him all the success in all the projects that he is working on.

Above that, we would like to thank "Dr. Abdelkader Hassein-Bey" for the efforts that he put into opening the branch of Nano-physics, which allowed us to access this amazing field of "Microsystems".In addition to this, we thank him for the efforts that he put into teaching us for longer hours every day, several days a week, all of this to deliver us valuable information that we certainly found helpful in the work reported in this thesis. Furthermore, we should thank him for co-advising us and bringing valuable help by providing us with innovative solutions and encouraging us when facing problems.

We would address our acknowledgements to the members of the jury, starting with the president of the jury "Mr. A.Benhaffaf", the examiner "Dr. N.Belgroune", and the advisors "Dr. A.Tahraoui" and "Dr. A.Hassein-Bey", for giving us the honor to examine this work, and for the time and efforts that they have taken to read and correct this manuscript.

We will certainly not forget all the teachers that taught us through all these academic years.

At last, it is more than a pleasure to address our acknowledgement to our family members, friends especially Sennoun Kahina; and every person that gave us material and emotional support, just to push us to study and reach this level.

TABLE OF CONTENTS

Abstract 1
Acknowledgements 2
Table of Contents 4
List of Figures 7
List of Tables 8
GENERAL INTRODUCTION 10
I. BACKGROUND 12
1. INTRODUCTION 5
2. SEMICONDUCTOR BASICS 5
2.1. Atomic Structure and Quantum Theory 5
2.2. Crystal Lattice 6
2.3. Energy Bands 8
2.4. Charge Carries 10
2.5. Doping 11
2.6. P-N Junction 11
2.7. PIN Junction 12
3.1. Origin of Solar Power 18
3.2. Solar Cell Characteristics 19
3.3. Solar Cell Input Power 21
3.4. Solar Cell Performance 23
4. CHAPTER SUMMARY 24
II. GaInP Properties 25
1. INTRODUCTION 26
2. DEFINITION OF III-V SEMICONDUCTOR MATERIALS 26
2.1. Ternary compounds: 27
3. IMPORTANCE OF III-V COMPOUNDS IN OPTOELECTRONICS 27
4. InGaP MATERIAL PROPERTIES 28
III. SILVACO ATLAS (TCAD) SIMULATION and RESULTS ....
1. INTRODUCTION 32
2. A BRIEF HISTORY ABOUT SILVACO 32
3. SILVACO (TCAD) SOFTWARE 33
4. ATLAS ENVIRONMENT 34
4.1. Atlas Operating Mode: 36
4.1.1. Syntax of an instruction: 36

4.1.2. Instructions' order:..37
4.2. Structure Specification:..38
4.2.1. MESHING..38
4.2.2. REGION..39
4.2.3. ELECTRODES..40
4.2.4. DOPING..41
4.3. Materials and Model Specification:..42
4.3.1. MATERIAL..42
4.3.2. MODELS..42
4.3.3. CONTACT..43
4.3.4. Numerical METHOD selection..43
4.4. Solutions Specification..44
4.4.1. Defining the light source..44
4.4.2. Obtaining solutions..45
4.5. Results' Analysis..46
1. INTRODUCTIO..47
2. RESULTS AND DISCUSSION..48
2.1. Evaluating Solar Cell's Electrical and Optical Properties..48
3. CHAPTER SUMMARY..50
III-V. GENERAL CONCLUSION.. 51
LISTOF SYMBOLS..52
REFERENCES..54

LIST OF FIGURES

Figure 1-1: The atomic structures for amorphous, crystalline, and polycrystalline materials [15] 7
Figure 1-2: The diamond lattice is shown with each black dot representing an individual atom and each solid line representing a bond between atoms. [15] 7
Figure 1-3: Inter-atomic distance is graphed against energy to show the formation of energy bands in a material. [16] 9
Figure 1-4: The relative bandgaps of insulators, semiconductors, and conductors are shown in Figures 4(a), 4(b), and 4(c) respectively. [16] 10
Figure 1-5: The junction between an n-doped and p-doped material forms a depletion region. Figure 5(a) shows majority carriers travelling across the junction due to the attraction caused by opposite charge carriers. The barrier caused by newly formed ions is shown in Figures 5(b) and 5(c). From [17] 12
Figure 1-6: p-and n layers band diagram. 13
Figure 1-7: electrons and holes density 15
Figure 1-8: carriers concentration 17
Figure 1-9: energy bands 18
Figure 1-10: electron flow in a solar cell 19
Figure 1-11: the tipical I-V curve for a solar cell that graphs anode voltage against cathode voltage 20
Figure 1-12: Spectral irradiance of the AM0g and AM1.5g spectrums 21
Figure 1-13: The spectral responses of gallium indium phosphide (GaInP), gallium arsenide (GaAs), and germanium (Ge) solar cells are graphed along with the AM0 spectrum. 23
Figure 2-1: Part from the periodic table with III-V elements highlighted in red ... 27
Figure 2-2: Bandgap values for different III-V compounds in function of their lattice constant 28
Figure 3-1: The Virtual Wafer Fabrication [15] 33
Figure 3-2: Inputs and outputs of Atlas [15] 34
Figure 3-3: DECKBUILD window 36
Figure 3-4: Order of groups of Atlas commands [15] 37
Figure 3-5: The structure of our GaInP pin solar cell that we want to simulate in SILVACO TCAD 38
Figure 3-6: The mesh statements creating the mesh for the GaInP P-I-N solar cell are displayed along with a picture of the created mesh 39
Figure 3-7: The region statements creating the regions of the GaInP P-I-N solar cell are displayed along with a picture of the created regions. 40
Figure 3-8: The cathode and the anode are made together with the electrode identification code in the GaInP P-I-N solar cell. 41
Figure 3-9: The I-V curve of a silicon solar cell as it is displayed in Tonyplot. ... 47
Figure 3-10: (a) (b) (c) and (d)represent the structures obtained for different i-layer thicknesses 48
Figure 3-11: (a) (b) (c) and (d) represent the I-V curves of our GaInP p-i-n solar cell with different i-layer thicknesses 49

LIST OF TABLES

Table 1-1:All possible values of all possible quantum numbers......................6

Table 2-1:nonzero bowing parameters for GaInP 29

Table 3-1:Results of the simulation for different parameters 49

GENERAL INTRODUCTION

Solar cell devices play an important role in renewable energies which convert solar energy directly into electricity. In recent years, tandem structures have been developed for high effi-ciency applications. These were stacked by multiple subcells with different band gaps to absorb the sun light in different spectral ranges and convert it into electric power. Multijunc-tion III-V tandem structure solar cells such as GaInP/ GaInAs/Ge triple junction cells have attracted increasing attention for their very high conversion efficiencies [1, 2]. However, the high cost of III-V tandem cells has been the main impediment for their widespread applications. Another kind of basic solar cell structures is p-i-n structure, which consists of p- and n-doped regions on top and bottom layers and an intrinsic layer (i-layer) in middle one. It provides a simple way to improve the absorption ability with a thick intrinsic region. It is also well known that the built-in electric field plays a critical role in solar cell devices; however, it is difficult to detect by electric methods directly and less studies have been reported [3]. In addition, the different thicknesses of an i-layer would be studied in detail because the thicker i-layer may induce more defects and lower the built-in electric field.

The first chapter describes the fundamentals of semiconductors and solar cells. In the third chapter, we explain in details the physical and properties of GaInP and P-I-N junctions.

The second chapter explains the fundamental properties of GaInP.

In the first part of chapter three, we explain SILVACO atlas software language and show how we should deal with this software. The second part deals with the simulation results.

Finally, this work has a conclusion that presents our results and a proposal for future work.

Chapter I

BACKGROUND

1. INTRODUCTION

The optoelectric properties of GaInP p-i-n solar cells with different intrinsic layer (i-layer) thicknesses from 0.25 to 1 m were studied in this thesis. To understand how **GaInP p-i-n solar cells** function, a basic understanding of semiconductor physics is required. The fundamental principles of semiconductor physics and solar cells are reviewed in this chapter.

2. SEMICONDUCTOR BASICS

Semiconductors are materials that can act either as an electrical insulator or conductor based on the conditions in which they operate. This behavior is due to the bonding properties of the individual atoms that form a bulk material and the interactions between their outer electrons. The individual atoms of semiconductors, like all other toms, have a set structure that determines how they will bond with other atoms.

2.1. Atomic Structure and Quantum Theory

An individual atom consists of positively charged protons, neutrons with no charge, and negatively charged electrons. It is held together by the attractive forces of the oppositely charged protons and electrons. The structure of an atom consists of a central nucleus composed of protons and neutrons that is orbited by a cloud of electrons. This electron cloud is made up of quantized shells that have an associated energy level. Every electron in this orbiting cloud must reside at a quantized energy level. An electron can move to a higher energy shell by absorbing energy or drop to a lower shell by releasing energy. This arrangement of electrons in the quantized shells is the most important determining factor in an atom's interactions with other atoms and, therefore, its electrical properties.

In every atom, each electron has a unique set of quantum numbers which describe its energy state in the atom. The four quantum numbers are represented by the letters n, l, m, and s. The first number n represents the shell that the electron occupies. Higher shell levels have electrons in higher energy states than lower shell levels. The l and m numbers denote subshells that appear within each shell and each can hold two electrons of4 opposite spin. The s number represents

the spin of the electron and can either be a positive or negative value. The possible values of each of the quantum numbers are summarized in Table 1.

Table 1-1. All possible values of all possible quantum numbers

Quantum Number	Possible Quantum Number Values
N	$n = (1, 2, 3, \ldots, n)$ where n corresponds to the energy level of the outermost shell
L	$l = (0, 1, 2, \ldots, n\text{-}1)$
M	$m = (-l, -l+1, \ldots, l\text{-}1, l)$
S	$s = (-1/2, +1/2)$

2.2. Crystal Lattice

Every solid material is made up of individual atoms organized in a certain manner and can be classified as amorphous, crystalline, or polycrystalline based on their arrangement. The basic lattice structure of amorphous, crystalline, and polycrystalline materials is shown in Figure 1-1. The most abundant solids found naturally on the earth are usually amorphous, meaning their individual atoms have no ordered arrangement. Contrastingly, a crystalline material is a material that has a periodic arrangement of atoms, called a crystal lattice, which is repeated throughout the solid. Therefore, the solid appears the same when examined at the atomic level at any point. Materials that do not fall into either the amorphous or crystalline category are classified as polycrystalline. These materials are composed of different regions that each have a periodic arrangement of atoms, but the whole material is not uniform in its arrangement.

charge carriers in the material, defining parameters such as resistivity and conductance. The arrangement of the atoms also determines whether certain materials can be grown in layers adjacent to one another to create a certain device. If two material lattice structures do not match in a certain manner, lattice mismatch will occur, a condition in which the lattices of two adjacent materials cannot create an appropriate electrical interface due to conflicting lattice structures. These properties governed by the crystal lattice combine with the properties and structure of the individual atoms to give every material unique properties.

2.3. Energy Bands

In much the same way that electrons can only reside at certain quantized energy levels in an individual atom, they are restricted to inhabiting energy bands in a solid. However, each of these energy bands is made up of a range of energy levels that each electron can occupy. This difference arises from the influence of all neighboring atoms on an electron. In the case of an individual atom, an electron resides in a quantized shell with an associated energy level. If two atoms are close enough to each other, their electrons and other attractive forces will influence each other, creating different energy states in specific bands of energy. In the band diagram in Figure 3, interatomic distance is graphed against electron energy. The band diagram shows that when atoms of the same element are infinitely far away from each other, they have the same quantized energy levels. However, when the atoms are closer together, the electrons of each atom interact, and the discrete energy levels diverge into a band of allowed energies shown by the grey portion of the graph in Figure 1-3.

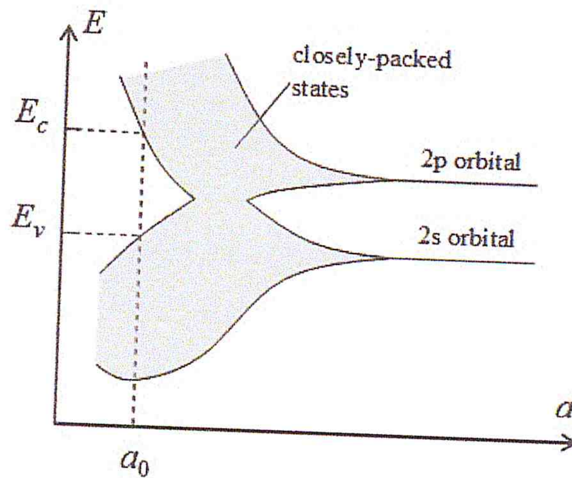

Figure 1-3: Inter-atomic distance is graphed against energy to show the formation of energy bands in a material [8].

The only energy bands of major concern in solar cell applications are the valence band and the conduction band. The valence band is the outermost energy shell of each atom. The electrons in this band are usually held in place by bonds between atoms. If an electron in the valence band receives energy greater than or equal to the difference in energy in the conduction and valence band, known as the bandgap, then it will move into the conduction band. When it moves into the conduction band, the electron breaks away from its bond and becomes a free electron in the material. An electron can only move up to the conduction when gaining energy in the valence band because there are no allowable energy states for an electron to occupy within the bandgap.

A material's ability to conduct electricity is highly dependent on its bandgap. Insulators have a relatively large bandgap and take a large amount of energy to excite free electrons. Semiconductors have a relatively small bandgap, allowing them to act as an insulating or conducting material dependent on the level of energy in the material. Conductors have overlapping valence and conduction bands and, therefore, have free charge carriers without the addition of outside energy. The differences in bandgap among insulators, semiconductors, and conductors are shown in Figure 1-4. The bandgap decreases as conduction ability increases.

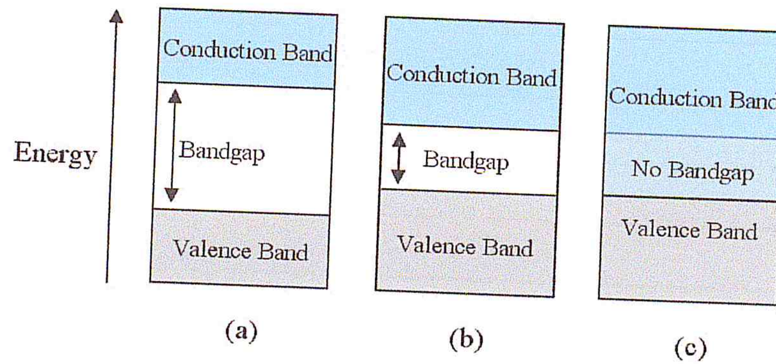

Figure 2-4: The relative bandgaps of insulators, semiconductors, and conductors are shown in Figures (a), (b), and (c) respectively [8].

Semiconductors have a moderate bandgap due to the unique conditions in their valence bands. All elemental or single element semiconductors have four electrons in the valence band of each atom. These elements are known as group IV elements. The atoms of these materials bond with each other to fill the outer shell of each of the surrounding atoms by the use of four covalent bonds with neighboring atoms. These covalent bonds can be broken by the introduction of energy, which frees charge carriers. Other semiconductors are made up of compounds in which the two element's valence electrons sum to eight. This can be achieved in many different elemental combinations to create effective semiconductor materials.

2.4. Charge Carries

When bonds are broken in a material due to the absorption of energy, two different types of charge carriers are created called electrons and holes. Electrons are simply the negatively charged elements of atoms and are considered free electrons when they break away from a bond. Holes are conversely the positive charge left behind by the broken bond of the free electron. Unlike free electrons, holes exist in the valence band. Holes are not physical particles but are merely positive charges created by the lack of necessary electrons for charge balance. Though holes are not physical particles with a mass, their flow is associated with a positive value of current while electron flow is associated with negative current.

Electrons and holes each have an associated mobility in every material based on how easily the free charge carriers can move through the material. Though electrons and holes are of equal charge, electrons have a higher mobility.

A material's electron and hole mobility are dependent on many material characteristics such as the lattice structure, the size of the atoms in the material, and the orientation of the channel in which the charge carrier is travelling. The electron and hole mobility determine parameters such as the conductance and resistivity of a material, which are important factors in solar cells.

2.5. Doping

Doping is the process of purposefully introducing impurities into a semiconductor material for the purpose of manipulating its electrical characteristics. A pure, undoped semiconductor is called intrinsic, while a doped semiconductor is called extrinsic. A semiconductor can be doped with either p or n type material. The p type dopants, called acceptors, have three or less valence electrons. This type of dopant bonds with all the surrounding atoms but lacks enough electrons to fully fill its outer shell. Thus, it attracts electrons, inducing the generation of holes in the material. An n type dopant, known as a donor, has five or more valence electrons, allowing it to fully bond with all of the neighboring atoms while leaving an extra, unbonded electron. This electron can easily be excited into the conduction band because it is not bound by the energy of a covalent bond. The extra charge carriers created by doping can greatly increase charge carrier concentrations, allowing for the fabrication of materials more suited to most applications than intrinsic semiconductors.

2.6. P-N Junction

Most of the applications of semiconductors, including solar cells, are possible due to the properties created by the junction between a p-type region and an n-type region. The region where these two materials meet is called a **p-n junction** and functions as a diode. In this region, excess electrons in the n region and excess holes in the p region diffuse across the border of the two regions to form a depletion region in which oppositely charged ions create a barrier that blocks charge flow. The formation of the depletion region from the junction of p-type and n-type materials is shown in Figure 1-5.

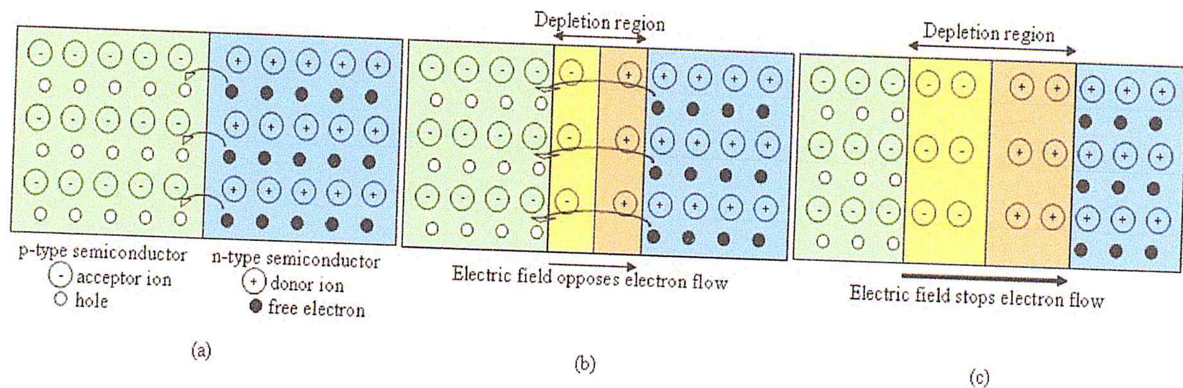

Figure 1-5: The junction between an n-doped and p-doped material forms a depletion region. (a) Shows majority carriers travelling across the junction due to the attraction caused by opposite charge carriers. The barrier caused by newly formed ions is shown in (b) and (c) [9].

The instant the materials meet, the excess carriers of each material border region move to the other side, attracted by the holes or electrons on the other side of the junction. These charges leave behind ions that then have a negative charge in the case of the p side and a positive charge in the case of the n side. This barrier then blocks charge flow because the electrons on the n side are repelled by the negative region on the edge of the n side and the opposite is true of the holes on the p side. If the junction is forward biased with a voltage greater than the potential of the depletion region potential, then the diode conducts current. If the diode is reversed biased, it acts as an insulator and the depletion region expands.

2.7. PIN Junction

The pin junction consists of three differently doped regions. As the name suggests, there is an intrinsic or undoped layer sandwiched between a p- and an n-doped region. Typically this kind of junction is fabricated from amorphous silicon with a band gap of about 1.8 eV. For the sake of simplicity, let us assume the same doping in the p- and in the n-layer. Using $N_a = N_d = 10^{18}$ cm^{-3} and an intrinsic carrier concentration $n_i = 10^{10}$cm^{-3}, we obtain the following band diagram. The p- and n-layers are represented by the flat bands to the left and right, respectively, and the intrinsic layer extends between 0 and 1 on the horizontal axis. Figure 1-6 shows the band diagram for p and n layers.

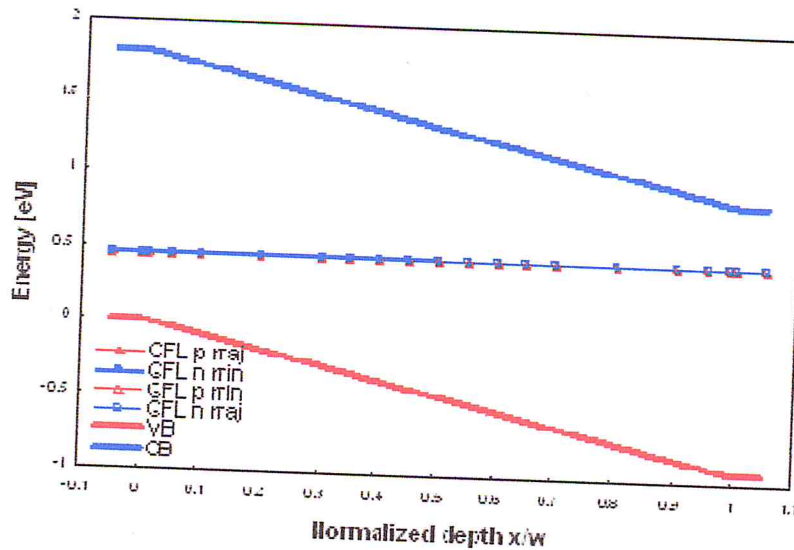

Figure 1-6: p- and n layers band diagram.

When all layers are in contact, the Fermi levels of the doped regions must align on the same height. This is shown by the horizontal line with symbols. Because there are no charges in the i-layer, the potential variation is just linear between the values that are fixed by the doped layers. The potential differece across the i-layer is **called built in potential V_{bi}**. It is calculated by subtracting from the band gap the values of the Fermi levels in the doped regions with respect to their band edges:

$$qV_{bi} = E_g - E_{F,n} - E_{F,p} \qquad (1)$$

Taking the relation for the Fermi level in a doped semiconductor from the chapter on doping, we finally find:

$$V_{bi} = \frac{KT}{q} 2ln \frac{\mathrm{Nd}}{ni} \qquad (2)$$

This yields a built in potental of about 900 meV, and in the doped layers the Fermi levels are located about 450 mV from the respective band edges using a typical band gap of 1.8 eV for amorphous silicon. Note that the term QFL in the legend is the abbreviatin of "Quasi Fermi Level". The "quasi" is not necessary here, but it will be used later.

So far the junction was in equilibrium. In operation the pin junction is contacted to an external electric circuit, and once it is illuminated we can draw a current. We would like to understand what goes on inside the cell. First of all we have to describe the properties of the charge carriers because in the end they make up the current.

We start by calculating the equilibrium charge carrier profile; from the previous sections we know that the introduction of charge carriers by doping can change the Fermi level with respect to the band edge. This is obviously the case for the p- and n-layers. In the intrinsic layer, however, the Fermi level is given, and we find that the valence band edge position linearly decreases with respect to the flat Fermi level. For the conduction band it is just the other way round. With given band edge and Fermi level, we can calculate the charge carrier profile throughout the i-layer by solving the above equation for the carrier density which is now unkonwn. For a position *x* between 0 an 1 we find the equilibrium profile of the carrier density:

$$n0(x)=\frac{ni^2}{Nd}e^{\frac{-qV\mathrm{bi}\ \mathrm{x}}{2a}} \qquad (3)$$

This yields an exponential increase of the electron concentration *n(x)* from 10^2 cm^{-3} to 10^{18} cm^{-3}, while at the same time the hole concentraton decreases exponentially from 10^{18} cm^{-3} to 10^2 cm^{-3}. The situation is illustrated in the figure below, where again the legend anticipates some considerations which will follow below.

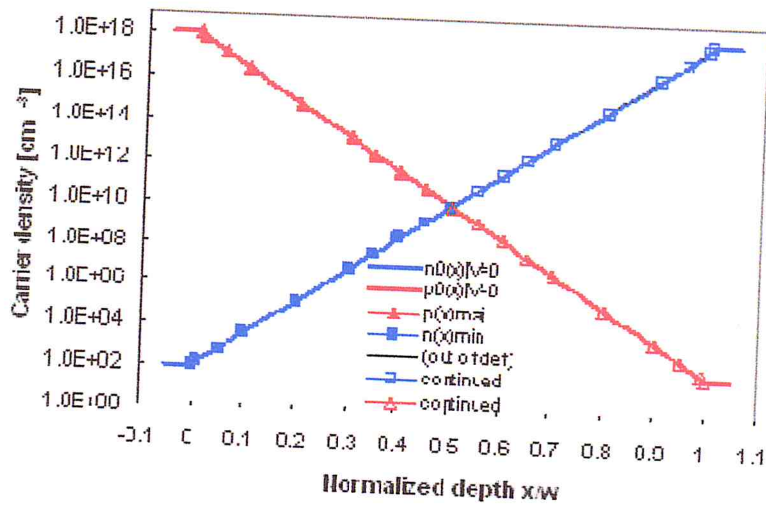

Figure 1-7: electrons and holes density.

An important observation emerges from the figure above; along the horizontal axis the hole density is higher than the electron density between 0 and 1/2, after that it is the other way round. We conclude that in the first part holes are the **majority carriers**, after that they are **minority carriers**. This is just a consequence of the mass action law, the product of n and p must equal n_i^2 at all places throughout the junction. The carrier densities of this situation are referred to equilibrium densities n_0 and p_0

The situation changes once we apply an electric bias to the cell. Under a forward bias V the potential drop throughout the cell decreases from the built in potential V_{bi} to $V_{bi}-V$. In the doped regions we have free charges which can follow the field and eventually cancel it out. Thus, the bands will stay flat like in metals, and the Fermi levels stay at their position inside the band gaps. In the intrinsic layer the bands still connect linearly between the doped regions, alas with a different slope. However, there emerges a problem with the Fermi level because it assumes different values at the opposite ends of the layer, it is longer unique. We can continue to use the convenient concept of the Fermi level if we split it into two separate relations, one for majority carriers and one for and minority carriers. These are called **Quasi Fermi Levels**, and generally it is assumed that the Fermi level for the majority carriers remains flat at a level equal to the one in the adjacent

doped region.

In the two halfes of the i-layer we can calculate the profiles of the two majority carrier densities just as above. The density of the minority carriers, however, must be determined by solving the continuity equation. The following is written down for electrons between 0 and 0.5, for holes it is just the same between 0.5 and 1.

$$G - R(x) + D\frac{d^2}{dx^2} + \mu F\frac{dn}{dx} = 0 \qquad (4)$$

The continuity equation takes care of the following processes:

- Generation of carriers: normally this takes place by by the absorption of light
- Recombination of excess carriers: every deviation from the equilibrium distribution n_0 is likely to recombine with a lifetime τ

$$R(x) = \frac{n(x) - n0(x)}{\tau} \qquad (5)$$

- Diffusion of carriers from places with high density towards places with lower density. According to the Einstein relation, the product of the diffusion constant D and the lifetime yields the square of the diffusion length$L$.

- Drift of carriers with a mobility μ along an electric field F

The result is a linear differential equation of second order with inhomogeneity. The solution is quite straightforward, but we must still define the boundary conditions; first, the carrier density at x=0.5 can be easily determined by using the reduced potential drop across the junction. Second, the drift current must equal the diffusion current. We specify this condition at x=0 because at a later stage it permits us to introduce recombination losses due to surface recomination. The figure below shows the result for the case of a foward bias of 0.4 V.

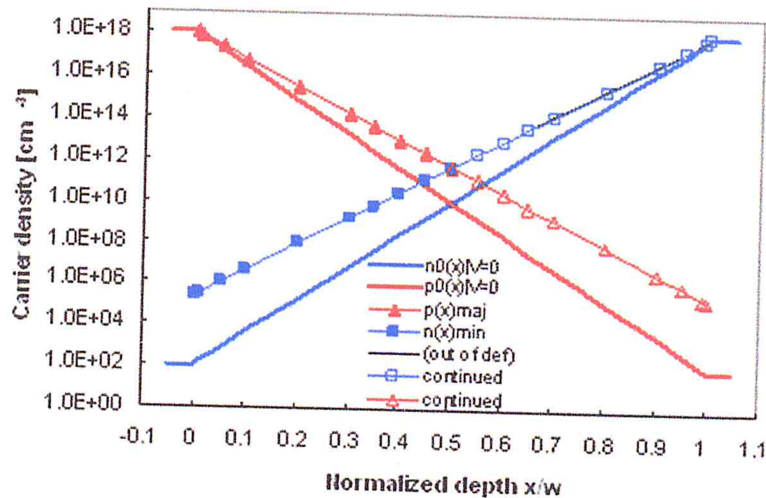

Figure 1-8: carrier concentration.

we should add a few words on the different curves that are shown: the first thing to calculate is the majority carrier concentration between 0 and 0.5, shown by the full red triangles. This is just the exponential drop due to the linear variation of the potential V_{bi} - V across the junction. This gives us the value for the bounary condition at x=0.5. We continute by calculating the solution of the continuity equation which gives the profile of the minority carrier concentration shown by the full blue squares. Then, we just mirror the relations into the second half, as shown by the open symbols. There is one more curve shown by a black line; this is the solution for the minority carriers between 0 and 0.5, but plotted beyond its range of validity into the range between 0.5 and 1. In fact, the curve is hardly different from the electron majority profile in this range, indicating that the the model is not that bad.

Having arrived at the carrier profiles across the junction, we would like to come back to the idea of the quasi Fermi level. We assumed them to be flat for the majority carriers, but we did not know their shape for the minority carriers. Knowing the minority profile and the linear variation of the band edges, we can easily calculate them. This is shown in the figure below, again for the case of 0.4 V forward bias; we observe that also for the minorities they stay essentially flat, but with a strong drop towards the contacts.

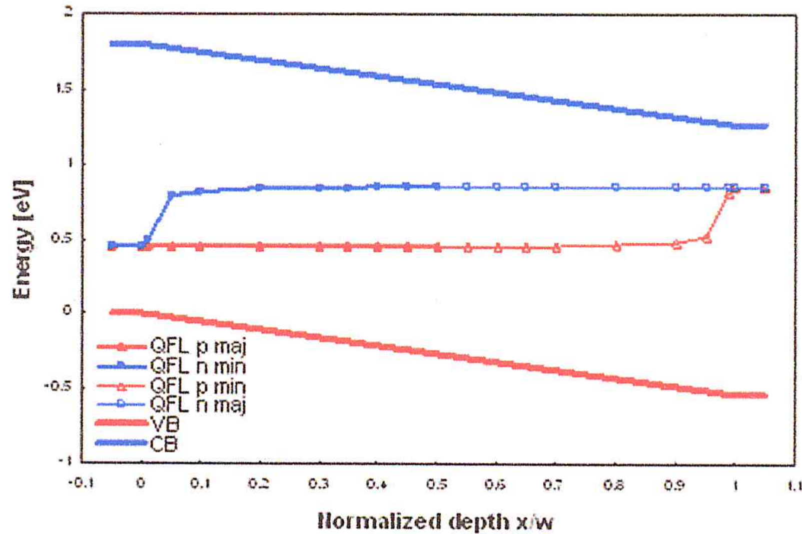

Figure1-9 : energy bands

3. SOLAR CELL OPERATION

Due to the properties of the p-n junction and the ability of semiconductors to absorb energy via photons of light, solar cells are able to generate power. The basic concepts behind solar power and the important characteristics that can quantify a solar cells performance are explained in this section.

3.1. Origin of Solar Power

A basic solar cell consists of a p-n junction with metal contacts on both sides of the junction. In an n on p solar cell the top n layer is called the emitter, while the bottom p side is called the base. When placed in an environment with light, the solar cell absorbs photons, which generate electron hole pairs near the depletion region. To generate power, the metal contacts to the emitter and base are tied together via an external load as shown in Figure 2-11. Due to the field of the depletion region, charge carries generated by photons are swept across the depletion region so that a photocurrent is generated in the reverse biased direction. However, when an external load is applied, the current induces a voltage across the load. This voltage induces a countering forward biased current that is less than the photocurrent but increases as the load reaches infinity. The net current in a solar cell is always in the reverse biased direction but decreases as

the forward biased current increases with an increasing load. The power produced by the cell is the product of the net current and voltage across the load.

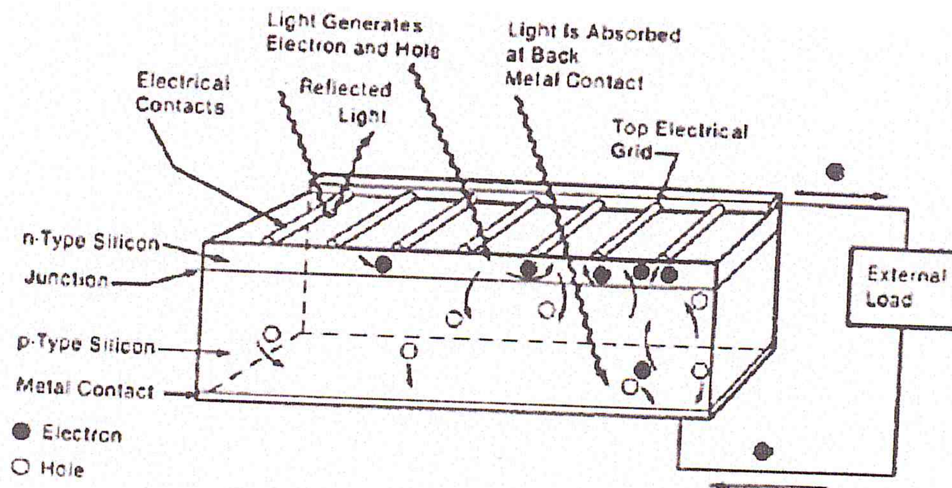

Figure1-10:electron flow in a solar cell(arrows denote electron flow) [10].

3.2. Solar Cell Characteristics

The most useful characteristic of a solar cell is its current-voltage (I-V) curve. This curve graphs the solar cell's net current per unit surface area in the y direction, against the associated load voltage in the x direction. A typical solar cell I-V curve is shown in Figure 1-11, which shows anode voltage plotted against cathode current. As discussed in the previous section, the value of load resistance affects both the load voltage and net current generated in the solar cell. The y intercept of the I-V curve is the limiting case in which there is no load resistance and a maximum value of current called the short circuit current (I_{sc}) occurs. In this case there is no induced voltage across the load, creating no forward biased current to counter the photon induced current. The x intercept represents the extreme case in which the load resistance is infinite, producing a maximum voltage known as the open circuit voltage (V_{oc}). In this case no current can flow due to the infinite resistance. Opposing charges are built up on both sides of the depletion region of the p-n junction, resulting in a maximum voltage across the infinite load. Though it is useful to know I_{sc} and V_{oc} for a solar cell, it is more useful to know the maximum power point (P_{max}). The maximum power current (I_{max}) and

voltage (V_{max}) can then be determined. These values show the actual power capability of a solar cell, the most important factor in the cell's application. The parameters V_{oc}, I_{sc}, Imax, and V_{max} are shown in Figure 1-11 on an I-V curve.

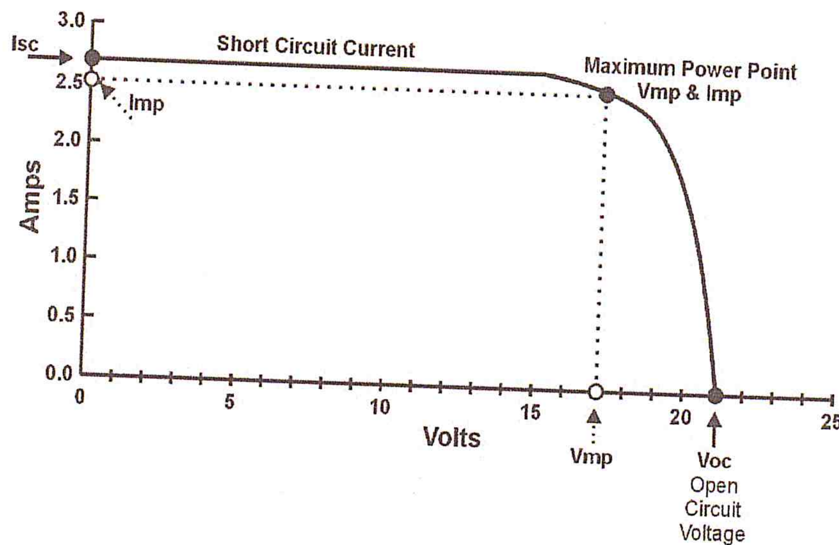

Figure 1-11: The typical I-V curve for a solar cell that graphs anode voltage against cathode current. V_{oc}, I_{sc}, I_{max}, and V_{max} are shown to display the limiting cases of the I-V curve and the maximum power point [11].

Once the I-V curve for a solar cell is determined, many parameters can be calculated which are useful in comparing the performance of different cells. Solar cell efficiency η is given by

$$\eta = \frac{P_{max}}{P_{in}} \times 100\% \qquad (6)$$

where P_{max} is the maximum achievable power of the solar cell and Pin is the input power from the light applied to the cell. The fill factor FF is given by

$$FF = \frac{P_{max}}{I_{sc}V_{oc}} \qquad (7)$$

where V_{oc} and I_{sc} are the open circuit voltage and short circuit current, respectively. The FF is a measure of how well a solar cell transfers its short circuit current and open circuit voltage properties into actual power. These two parameters are useful for comparing solar cells but are dependent upon the input power to the solar cell, which varies based upon the light source applied.

3.3. Solar Cell Input Power

The input power to a solar cell is dependent upon the light source in which the cell is operating. In this thesis, air mass 1.5 (**AM1.5**) is used. Solar panels do not generally operate under exactly one atmosphere's thickness: if the sun is at an angle to the Earth's surface the effective thickness will be greater. Many of the world's major population centres, and hence solar installations and industry, across Europe, China, Japan, the United States of America and elsewhere (including northern India, southern Africa and Australia) lie in temperate latitudes. An AM number representing the spectrum at mid-latitudes is therefore much more common. "AM1.5", 1.5 atmosphere thickness, corresponds to a solar zenith angle of z=48.2°. While the summertime AM number for mid-latitudes during the middle parts of the day is less than 1.5, higher figures apply in the morning and evening and at other times of the year. Therefore, AM1.5 is useful to represent the overall yearly average for mid-latitudes. The specific value of 1.5 has been selected in the 1970s for standardization purposes, based on an analysis of solar irradiance data in the conterminous United States. [12] Since then, the solar industry has been using AM1.5 for all standardized testing or rating of terrestrial solar cells or modules, including those used in concentrating systems. The latest AM1.5 standards pertaining to photovoltaic applications are the ASTM G-173 and IEC 60904, all derived from simulations obtained with the SMARTS code.

Figure 1-12 shows the corresponding spectral irradiance for AM1.5 light beam compared with AM0 (full spectrum) spectral irradiance light beam.

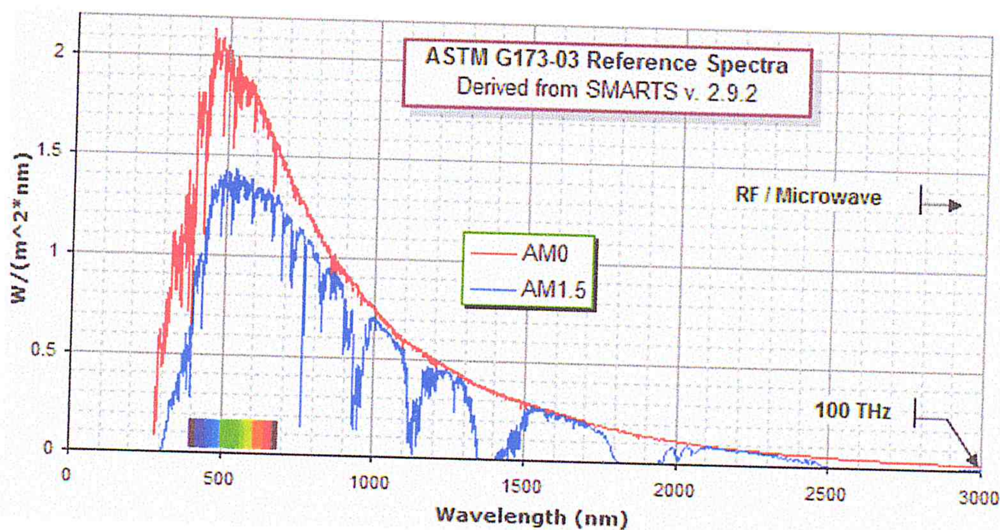

Figure 1-12: Spectral irradiance of the AM0g and AM1.5g spectrums [13].

Due to the properties of solar cells, only part of the solar spectrum can be converted into electrical power. This is caused by the different bandgaps and optical properties of materials. The bandgap of a material determines the minimum amount of energy required to generate an electron hole pair in the material. Any photon with energy less than the bandgap will simply pass through the material without exciting an electron. The energy of a photon is dependent on its wavelength and is given by

$$E = \frac{1.24}{\lambda} \qquad (8)$$

where E is in units of eV and λ is the wavelength of the photon in μm. The shorter the wavelength of a photon, the higher its energy and ability to generate electron hole pairs in higher band gap materials.

Though it would seem that lower band gap materials would have the ability to harness the widest range of photons, photons with energies much greater than the band gap of a material are not very efficient at generating electron hole pairs. To easily display a solar cell's response to photon energy, a spectral response curve graphs photon wavelength against the efficiency of charge carrier generation. Different materials have different curves that are limited to a maximum wavelength based on the material band gap and a threshold at which photons have too much energy. In this thesis, the mid-level band gap material gallium arsenide (GaAs) is used. GaAs has a spectral response which indicates efficient charge carrier generation by photons ranging in wavelength from 0.6μm to 0.9μm as seen in Figure 1-13.

Frequency response

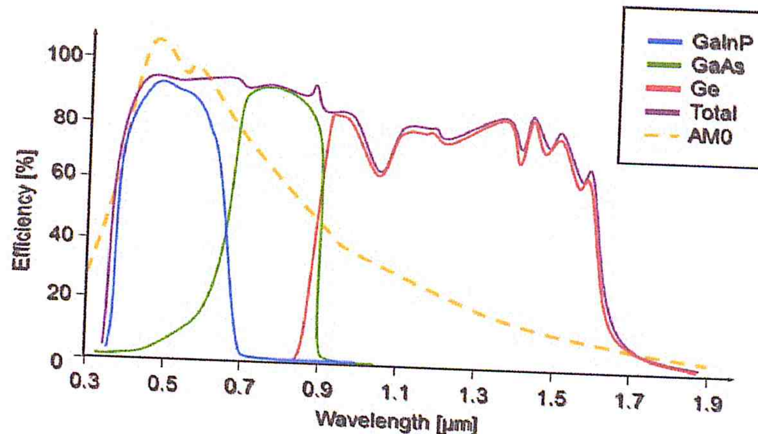

Figure 1-13: The spectral responses of gallium indium phosphide (GaInP), gallium arsenide (GaAs), and germanium (Ge) solar cells are graphed along with the AM0 spectrum [11].

3.4. Solar Cell Performance

Though solar cell performance is largely dominated by a material's spectral response and I-V characteristics, there are many other factors that influence a solar cell's performance. The more important factors that affect solar cell performance are:

- The reflection of light off the surface of a solar cell limits the amount of input power into the cell. The optical properties of different materials cause a portion of the photons hitting the solar cell to be reflected off the surface. This can cause a 35% loss in the theoretical efficiency of a solar cell without the use of antireflective techniques [11].
- Photons with energy much higher than the band gap generate electron hole pairs, but the excess energy is dissipated as heat in the crystal lattice of the solar cell. Low energy photons that do not generate charge carriers also bombard the atoms in the crystal lattice and create heat. This heating causes a loss in the voltage of a solar cell. A solar cell loses 2mV/K in voltage, which can drastically lower the efficiency of a solar cell [11].
- Recombination of electrons and holes can cause the charge carriers generated by photons to meet in the lattice and cancel each other out. When this happens, a free electron meets with a hole in the valence band

and occupies that space, no longer contributing to the number of charge carriers in the solar cell [11].

- Material defects in the solar cell can create traps which create more recombination. Cheaper, less pure materials can have significant defects that negate much of the generated current [11].
- The resistance of the bulk material causes a voltage drop within the solar cell that reduces the efficiency. When charge carriers are generated, they have to travel to the contacts of the solar cell to be harnessed as energy. The distance travelled through the lattice is often relatively great for each charge carrier, creating a high resistance seen by each of the charge carriers. This decreases the net voltage seen at the contacts [11].
- Shading from the top electrical contact completely blocks light to portions of the solar cell. The optimal top contact grid usually covers 8% of a solar cell. This 8% of the solar cell surface receives no photons to generate charge carriers and does not contribute to the power production of the solar cell [10].

4. CHAPTER SUMMARY

The background in semiconductor physics and solar cells necessary to understand the research in this thesis was provided in this chapter. The basic properties of semiconductors the theory and P-IN junction were shown to be optimal for generating solar power. The ability to generate electron hole pairs by the absorption of photons with energy greater than the bandgap allows solar cells to deliver power to a load. The producible power was shown to be dependent on both the material of the solar cell and the spectrum of input light. The power was also shown to be limited by factors inherent in the real properties of fabricated solar cells.

Chapter II

GaInP Properties.

II.I InGaP MATERIAL PROPERTIES

1. INTRODUCTION

In the set of materials, semiconductors constitute a well-defined class, with particular physical properties that are sources of interest in terms of fundamental knowledge and applications. These two unseparated factors make the importance of these materials, despite the limited number of elements and semiconductor compounds.

Mainly remarkable for their electronic properties, semiconductors are used in almost all electronic and optical equipment. The biggest part of the components (transistors, diodes, and so-called chip in general) are made of silicon, which plays a preponderant role, its technology and its theoretical knowledge have reached unmatched levels.

In fast electronics and optoelectronics, the properties of silicon are insufficient (mobility of relatively small carriers and indirect electronic transitions at the optical absorption threshold). In such applications, the III-V semiconductor compounds are preferable. The properties of these materials are very advantageous for the performances of these devices.

Among these semiconductors, we find mainly the gallium-indium phosphide (InGaP) which is at the center of this work. This material is a semiconductor belonging to the category of III-phosphides, that is to say, composed of nitrogen and elements of column III of the Mendeleev table, namely boron, aluminum, Gallium, indium and thallium. Gallium-indium phosphide is an alloy between gallium nitride (GaN) and indium nitride (InN). Therefore, we will mainly define the III-V semiconductors and then describe the properties of these two binary alloys (GaN) and (InN), and then describe the properties of the InGaN resulting from them.

2. DEFINITION OF III-V SEMICONDUCTOR MATERIALS

III-V semiconductor materials are compound bodies formed from an element of column III and an element of column V of the table of the Mendeleev

periodic table (figure 2-1). Thus, many binary, ternary and quaternary compounds can be produced.

IIB	IIIA	IVA	VA	VIA
	B Boron	C Carbon	N Nitrogen	O Oxygen
	Al Aluminum	Si Silicon	P Phosphorus	S Sulphur
Zn Zinc	Ga Gallium	Ge Germanium	As Arsenic	Se Selenium
Cd Cadmium	In Indium	Sn Tin	Sb Antimony	Te Tellurium
Hg Mercury	Tl Thallium	Pb Lead	Bi Bismuth	Po Polonium

Figure 2-1: Part from the periodic table with III-V elements highlighted in red

2.1. Ternary compounds:

III-V ternary alloy systemsare potentially of great importance for many high-speed electronic and optoelectronic devices; because they provide a natural means of tuning the magnitude of forbidden gaps so as to optimize and widen the applications of such semiconductors. Literature on the fundamental properties of these material systems is growing rapidly. In a ternary alloythe bandgap energy *Eg* and the lattice parameter a are generally both functions of a single composition parameter; so they cannot be selected independently.

3. IMPORTANCE OF III-V COMPOUNDS IN OPTOELECTRONICS

III-V compound semiconductors (SC) have played a crucial role in the development of optoelectronic devices for a broad range of applications. Major applications of InP or GaAs based III-V compound SC are devices for optical fiber communications, infrared and visible LEDs/LDs and high efficiency solar cells. GaAs based compounds are extremely important for Photovoltaic Solar Cell applications. We review its parameters later in this work.

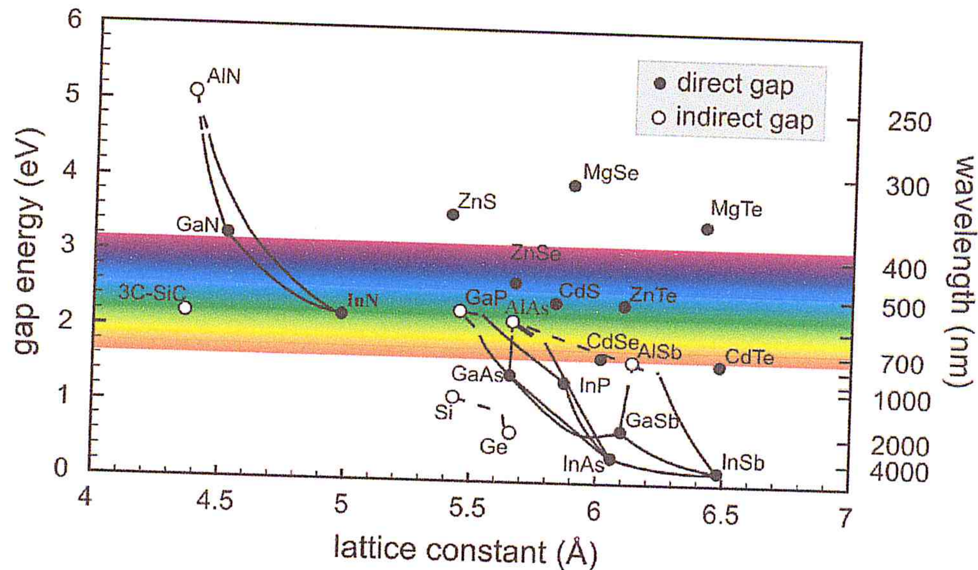

Figure 2-2: Bandgap values for different III-V compounds in function of their lattice constant [14].

4. InGaP MATERIAL PROPERTIES

The InGaP alloy exhibits some of the largest direct gaps among the non-nitride III-V semiconductors. Furthermore(Ga0.51In0.49P ~Eg51.9 eV at 300 K) is lattice matched toGaAs, which makes it an attractive material for wide-gap GaAs-based quantum well devices such as red diode lasers. This application has spurred extensive studies of the band structure characteristics of GaInP, which are at present rather well known.

For the G-valley band gap, early photoluminescence and cathodoluminescency determinations yielded bowing parameters ranging from 0.39 to 0.76 eV Subsequent electroreflectance and modulation spectroscopy studies favored a value near the higher end of that range. Theoretical studies have also produced a wide range of bowing parameters, with the most reliable results clustered around 0.5–0.75 eV. By analogy to GaInAs and AlInAs, it is useful to consider the $Ga_{0.51}In_{0.49}P$ alloy for which the most extensive data are available. Unfortunately, a precise measurement for this lattice-matched alloy is somewhat complicated by its proximity to the indirect crossover point, and by long-range ordering of the group-III atoms which can take the form of a monolayer InP–GaP superlattice along the [111]. direction. The ordering-inducedreduction of the direct energy gap can be on the order of 100 meV. Low-temperature band gaps of 1.969–2.018 eV have been

reported for random GaInP alloys that are nominally lattice matched to GaAs. Using the result of Emanuelsson *et al.*, corrected for the exciton binding energy of 8 meV, we obtain a recommended bowing parameter of C50.65 eV. That value is consistent with recent data for nonlattice-matched compositions. The *X*-valley gap energies in InP and GaP are nearly equal (2.38 and 2.35 eV, respectively, at 0 K), and the

G–*X* crossover composition in GaInP is believed to be close to *x*=0.7.

TABLE 2-1 . Nonzero bowing parameters for GaInP.

Parameters	Recommended values	Range
Eg (eV)	0.65	0.39 - 0.76
E_g^X (eV)	0.20	0 - 0.39
E_g^L (eV)	1.03	0.23 – 0.86
D_{so} (eV)	0	-0.05 - 0
m_e^* (G)	0.051	......
F	0.78	......
d (eV)	0	0 – 2.4

Although early work usually assumed a linear variation of the *X*-valley gap, Auvergne *et al.* have more recently suggested $C(E_{gX})$50.147 eV on the basis of piezoreflectance spectroscopy in the composition range near the crossover point. Somewhat larger bowing parameters are implied by the pressure experiments of Goni *et al.* and Meney *et al.* Our recommended value of $C(E_{gX})$50.2 eV agrees with other experimental and theoretical results.

Early experimental and theoretical determinations of the bowing parameter for the L-valley gap were summarized by Bugajski *et al.*The Gamma– *L* crossover most likely occurs at *x* slightly smaller than the G–*X* crossover point, which makes *L* the lowest conduction valley for *x* greater than 0.67. Krutogolov *et al.*suggested

$C(E_{gL})$50.71 eV, although that article assumed *L*-valley indirect band gaps in the end-point binaries that are considerably different from the ones adopted here.

Modeling of the ellipsometric and thermoreflectance data of Ozaki *et al.* yielded E_{gL} =2.25 eV in $Ga_{0.5}In_{0.5}P$ at 300 K, which favors a small *L*-valley bowing. In deriving our recommended bowing parameter,we employed the G– *L* crossover point of *x*=0.67, which was confirmed recently by Interholzinger *et al.* The bowing of the spin-orbit splitting in GaInP is known to be very small, with recent results implying a linear interpolation to within experimental uncertainty

The electron effective mass in a random alloy with *x*=0.5 was measured by Emanuelsson *et al.* to be m_e*=0.092m_0, which is somewhat lower than the linearly interpolated values quoted in other papers. Similar results were obtained by Wong *et al.* In the absence of reliable data for the other electron and hole masses, linear interpolation is advised using the scheme outlined above. With a linearly interpolated value of E_P=26 eV for the interband matrix element in $Ga_{0.5}In_{0.5}P$, we derive an *F* parameter of -1.48, and from it the corresponding bowing.

The shear deformation potential *d* was measured for GaInP grown on GaAs(111)*B* substrates. While the results imply a bowing parameter of 2.4 eV, the large uncertainties in existing determinations make it difficult to conclusively prefer this value over a linear interpolation .

Chapter III

SILVACO ATLAS (TCAD) Simulation and Results

III.I. SILVACO ATLAS (TCAD) SIMULATION TOOL

1. INTRODUCTION

In our work, we used technological simulation software **SILVACO (TCAD)**, to simulate the electrical and optical characteristics of a **InGaP P-IN solar cell**. First, we should learn some basic notions about simulation in general and this software and particularly using examples illustrating the work, and then we would proceed to our simulation and discuss the results that we obtained from our work.

The Role of Simulation

The simulation offers a link between the experimental world and the theoretical one, as it complements theory and experiment and builds physical reality in the presence of certain constraints or the presence of an impossible mathematical analysis.

2. A BRIEF HISTORY ABOUT SILVACO

SILVACO (Silicon Valley Corporation) is an American company, headquartered in Santa Clara, California. It is a leading provider of professional chains of finite element simulation and computer-aided design software for the Technology Computer Aided Design (TCAD) technology. These tools are used by microelectronics companies in the field of research, development and design of devices

Historically the company was founded in **1984** by **Dr. Ivan Pesic** to meet the needs of integrated **IC** designers for increasingly accurate and linear Simulated Programming with Integrated Circuit Emphasis (SPICE) models.

The entry of **SILVACO** into **TCAD** technology took place in **1989,** and wasbased on a research of the Department of Physical Devices of StanfordUniversity, thus appear in **SILVACO "Athena"** as process simulator and **"Atlas"** As a simulator of the devices (2D and 3D).

SILVACO has not been designed to meet a single semiconductor component. By including more general models of semiconductor physics, it allows

for more extensive simulations by scanning a whole range of electronic components.

3. SILVACO (TCAD) SOFTWARE

The VWF: (virtual wafer Fab):

Among the various software that it forms the VWF are the two most famous used ATHENA and ATLAS, these tools are divided into two main categories.

- **Main Tools** and **Auxiliary tools**

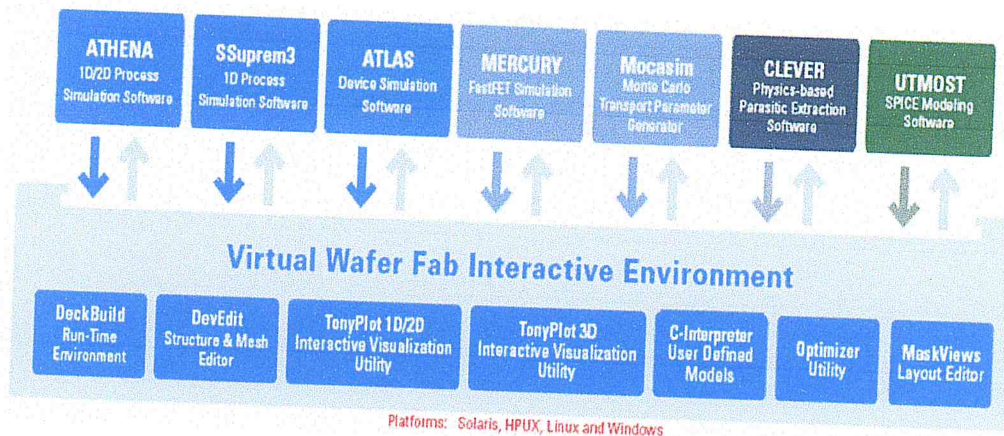

Figure 3-1:The Virtual Wafer Fabrication [15]

ATLAS is an electronic simulator capable of predicting the electrical characteristics of most semiconductor components in continuous, transient or frequency regime. In addition to the "external" electrical behavior, it provides information on the internal distribution of variables such as carrier concentrations, electric field or potential, etc., all important data for the design and optimization of technological processes.

This is accomplished by numerically solving the Poisson's equation and the continuity equations of the two-dimensional electrons and holes in a finite number of points forming the mesh of the structure defined by the user or by another program.

ATLAS has been designed so that it can be used with other tools that facilitate or supplement its use.

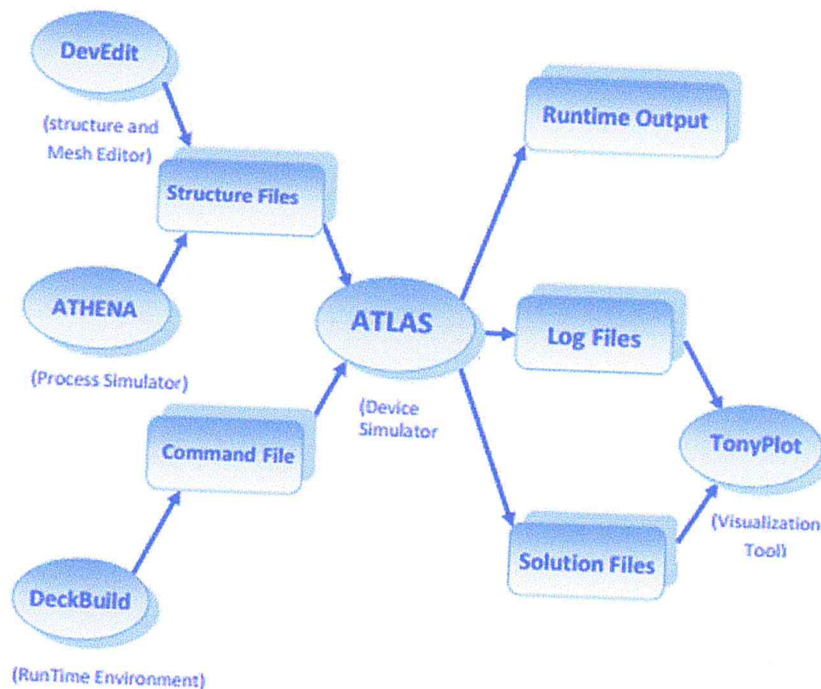

Figure 3-2: Inputs and outputs of Atlas [15].

4. ATLAS ENVIRONMENT

ATLAS is an electronic simulator capable of predicting the electrical characteristics of most semiconductor components in continuous, transient or frequency regime. In addition to the "external" electrical behavior, it provides information on the internal distribution of variables such as carrier concentrations, electric field or potential, etc., all important data for the design and optimization of technological processes.

This is accomplished by numerically solving the Poisson's equation and the continuity equations of the two-dimensional electrons and holes in a finite number of points forming the mesh of the structure defined by the user or by another program.

This simulator consists of two parts:

- A Digital Processing Part (method of integration, discretization ...),
- A part formed of the physical models of the most recent semiconductor components: models of recombination, impact ionization, mobilities, temperature and statistics of Fermi-Dirac and Boltzmann in particular.

The diagram in Figure 4.2 shows the different types of information that circulate at "**Atlas**" inputs and outputs. Most simulations carried out under "Atlas" use two input files. The first file is a text file containing commands for "**Atlas**" to run (represented by "Command File"). The second file is a "structure file" containing the structure of the device to be simulated defined in "**Athena**" or "**DevEdit**".

At the "Atlas" output, we have three types of files. The first of these files is the "**Runtime**" output, which gives progress, errors and warning messages during the simulation. The second type of file is the "**log**" file, which stores all voltage values and currents from the analysis of the simulated device (this is the file of the electrical behavior). The third output file is the "**Solution File**", this file stores the 2D or 3D data concerning the values of the solutions variables at a given point of the device.

ATHENA is a simulation software including in SILVACO and is used for simulating the manufacturing process of the different constituents of an electronic device, and also treats ion implantation and diffusion of impurities and oxidation and other technological processes of manufacturing. It is generally used to simulate simultaneously With Atlas.

DEVEDIT is an environment where the structure (dimension, doping, ...) and its mesh are drawn.

DECKBUILD is an environment where the simulation program is defined as shown in Figure 3-3.

TONYPLOT is an environment where the simulation results are displayed (structure of the component, distributions of various quantities in it, electrical characteristics ...).

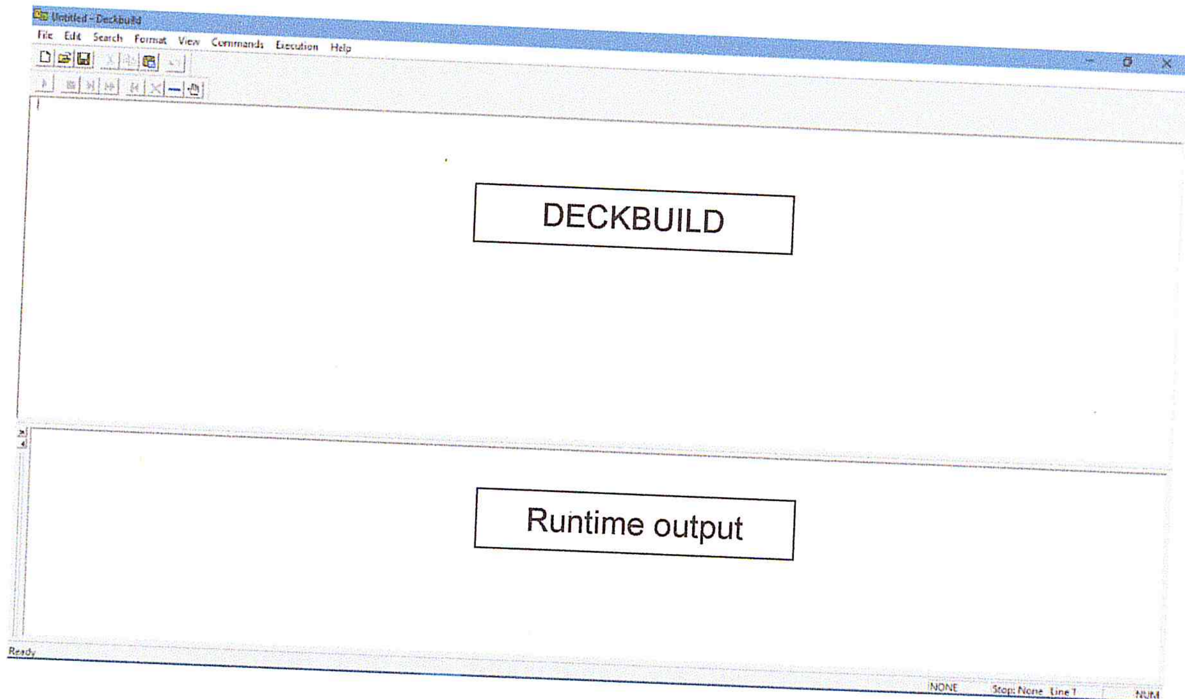

Figure 3-3: DECKBUILD window.

4.1. Atlas Operating Mode:

The command is entered in DECKBUILD by **go atlas**.

4.1.1. Syntax of an instruction:

An instruction takes the following general form:

```
<Instruction><parameter> = <value>
```

There are 04 types for values (real, integer, logic, character)

The order of parameters is not mandatory; abbreviation is possible but requires no overlap with other instructions.

To write a comment that is not executed by the compiler, we use the symbol **#**.

ATLAS can read **256** characters in a line, but it is better to separate the lines with a backslash at the end of the line in a long statement so that the instructions can be read in a clear way.

It does not differentiate between a capital letter and a lowercase letter.

The following figure represents the structure of the GaInP P-I-N solar cell that we want to simulate in ATLAS.

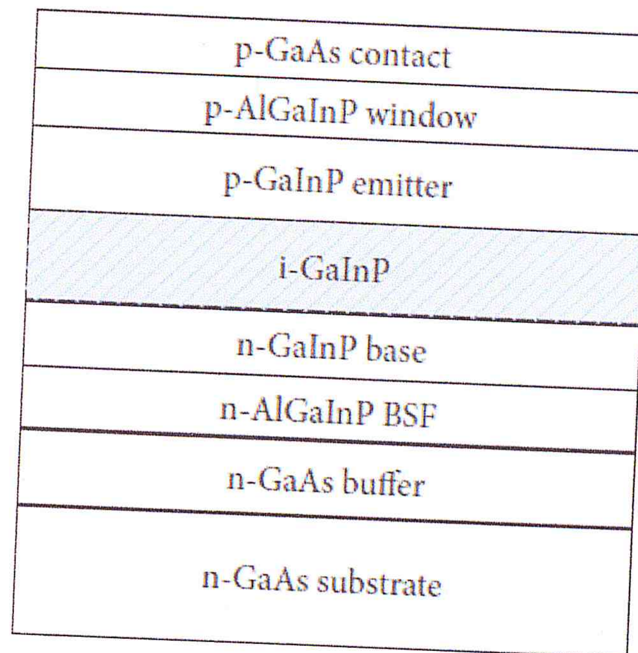

Figure 3-5: The structure of our GaInP P-I-N solar cell that we want to simulate in SILVACO TCAD.

4.2. Structure Specification:

The specification of the structure is obtained by identification of **mesh, regions, electrodes and the doping.**

4.2.1. MESHING

The first section of structure defining statements in the Deckbuild program is the meshing section. This section specifies the two-dimensional grid that is applied tothedevice with mesh statements.

The following instruction is used to define the meshing:

```
x.mesh location=<value> spacing=<value>
```

The ATLAS device simulator can more easily solve the differential equations at each grid point if there are no abrupt changes between adjacent points. Mesh statements have two parts called location statements and spacingstatements.

The location statement, "loc", specifies the x or y value in the structure to whichthe following "spacing" statement is applied.

The spacing statement, "spac", specifies thespacing between grid lines at that specific location.

TheFigure 3-6 represents the meshing that we have created for our structure and its respective instructions entered in DECKBUILD.

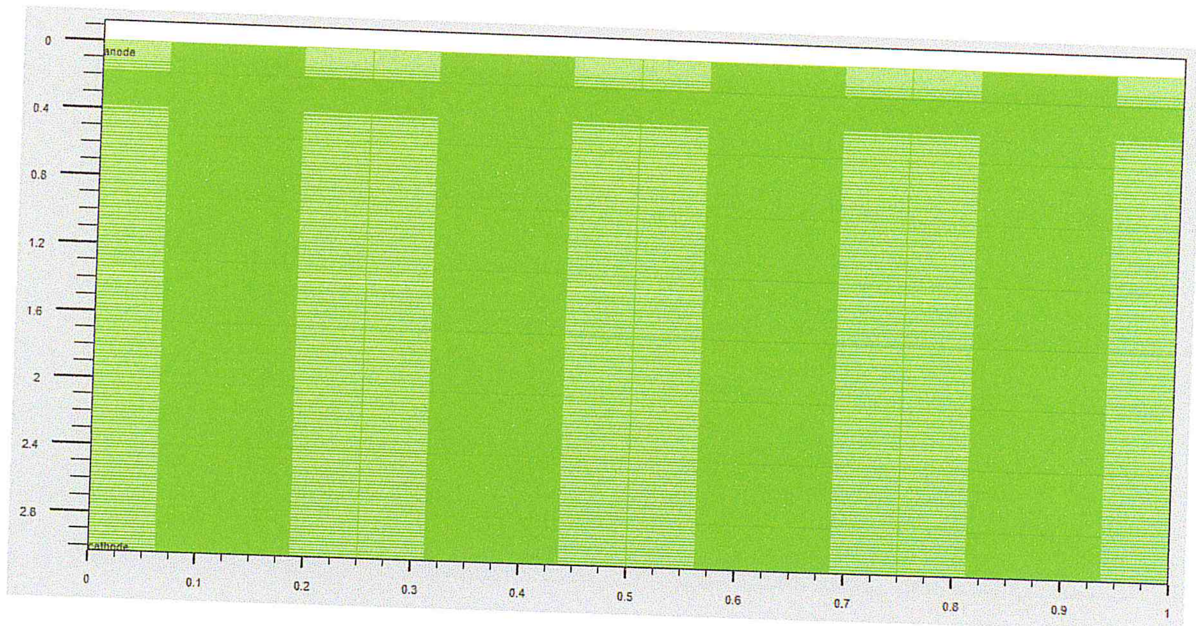

Figure 3-6: The mesh statements creating the mesh for the **GaInP P-I-N** solar cell are displayed along with a picture of the created mesh

4.2.2. REGION

The region statements include a region number, a material specification, and the region boundaries. The region number is arbitrary but is used in later structure specification sections to apply characteristics to certain regions.

The instruction for defining regions is as follows:

```
REGION     number=<integer>     material=<material_type>     /
<position_parameters>
```

Every region must have a different number as the program produces an error if a statement applies to two different regions.

The material specification statement specifies that the whole region consist of the stated material. This statement gives that whole region default parameters and characteristics of that specified material, which are stored in the **ATLAS material library**. These values include parameters such as the bandgap, electron and hole mobility, and optical properties such as the index of refraction.

P.S: These parameters can be used or changed in another section of the structure defining code if the user wishes to modify a material's original properties.

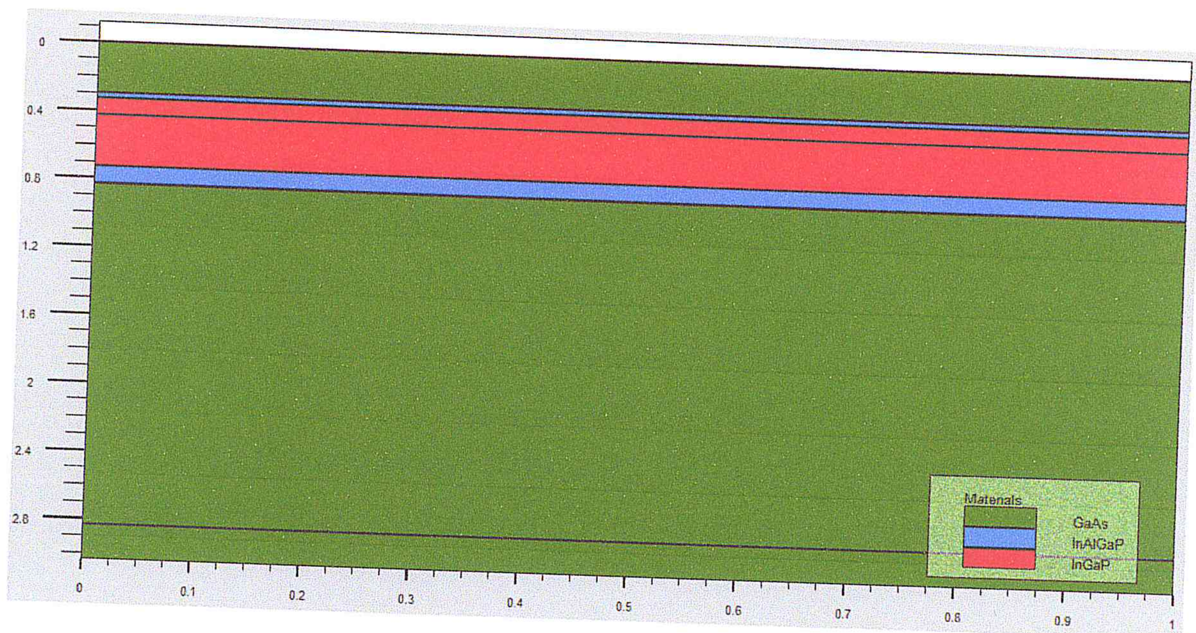

Figure 3-7: The region statements creating the regions of the GaInP P-I-N solar cell are displayed along with a picture of the created regions.

4.2.3. ELECTRODES

The definition of electrodes is as follows:

```
Electrode Name=<Electrode Name><position_parameters>
```

The user has the ability to determine any number of electrodes with different metal properties. Each electrode definition statement usually has three parts. The user must first name each pole. The name can be followed by the "material" statement, which is used to determine the type of contact metal that is used as electrode, which can be one of the materials registered in ATLAS Material Library, or a user-defined material.

The statement for the definition of an electrode uses maximum and minimum limits of x and y values to set the limits of each electrode. The positions of the electrodes are located by the following instructions:

`X.MIN`: Specifies the starting point of the electrode.

`RIGHT`: the position of the electrode is located to the right of the structure (inverse: `LEFT`).

`TOP`: the position of the electrode is at the top of the structure (inverse: `BOTTOM`).

It is also possible to name the electrode only and identify it as covering the top or the bottom of solar cells.

In our example two anodes at the top of the structure with a length of 2 µm each, and a cathode at the bottom of the structure translated by the following instructions in Figure 3-8

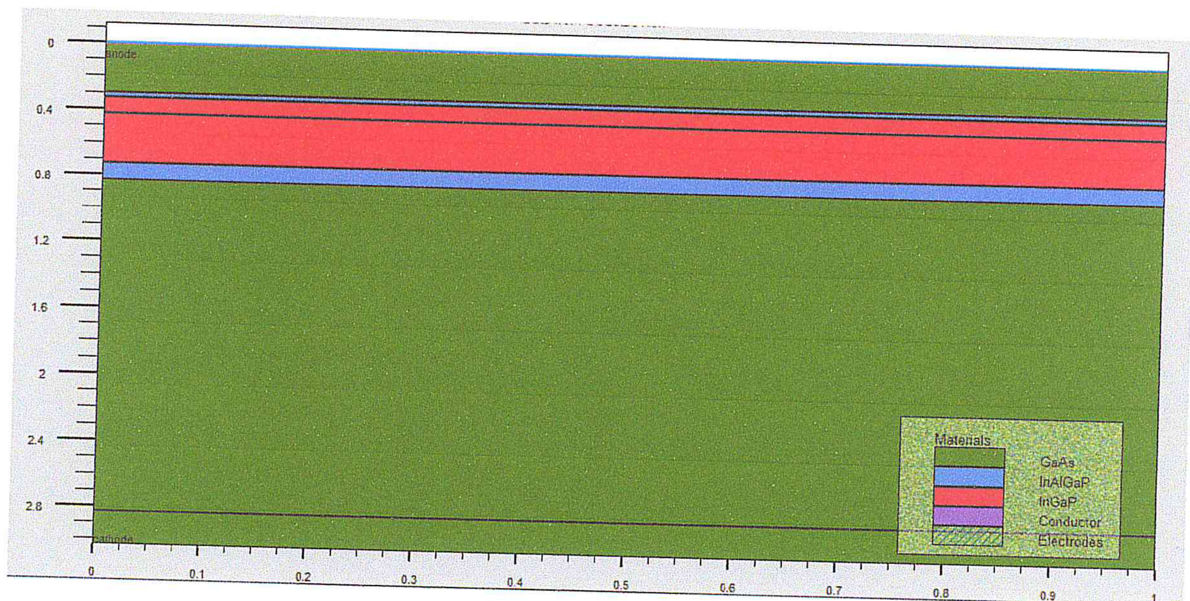

Figure 3-8: The cathode and the anode are made together with the electrode identification code in the GaInP P-I-N solar cell.

4.2.4. DOPING

The last aspect of structure specification that needs to be defined is doping. The format of the Atlas statement is as follows:

```
DOPING <distribution type><dopant_type><position parameters>
```

4.3. Materials and Model Specification:

After specifying the mesh and doping, we can easily modify the characteristics of the materials used (electrodes, substrate) and change their parameters that ATLAS takes them by default and define our choice of the physical model that will be used during the simulation. These actions are accomplished by the following instructions: MATERIAL, CONTACT, and MODELS.

4.3.1. MATERIAL

The material defining statements that follow the definition of the device structureallow the user to alter the properties of given materials or to input newmaterials into the device. The statements alter the material properties of a specifiedmetal, semiconductor, or insulator, to simulate more accurately a device that uses materials that do not match the given default values of the ATLAS software and the format for the material statement is as follows:

```
MATERIAL <localization><material_definition>
```

Different parameters can be defined with different material statements. Examples include the bandgap at room temperature (EG300), electron and hole mobilities (MUN and MUP), recombination parameters (TAUN and TAUP), etc.

In our example, we used GaInP and GaAs as basic materials in building the structure. The following statements are used to define their properties.

```
Material material=GaAs EG300=1.42 NC300=4.35e17 /
NV300=8.16e18 MUN=8000 MUP=400
```

For GaAs, we have overridden its ATLAS Material Library parameters and gave it different ones, to obtain results that are more accurate.

4.3.2. MODELS

The physical models fall into five categories: mobility, recombination, carrier statistics, impact-ionization, and tunneling. The syntax of the model statement is as follows:

```
MODELS <model flag><general_parameter> /
<model_dependent_parameters>
```

The choice of model depends on the materials chosen for simulation. The example below activates several models.

```
MODELS CONMOB FLDMOB SRH
```

CONMOB is the model for the concentration dependent mobility.

FLDMOB is the model of Dependence of the electric field.

SRH is the Shockley-Read-Hall model.

4.3.3. CONTACT

Contact determines the physical attributes of an electrode: anode, cathode, drain, etc. The syntax for contact is as follows:

```
CONTACT NUMBER=<n> |NAME=<name>|ALL
```

Here is our example of a contact statement:

```
contact name=anode workfunction=3.5
```

4.3.4. Numerical METHOD selection

After the materials model specification, the numerical method selection must be specified. There are various numerical methods to calculate solutions to semiconductor device problems. There are three types of solution techniques used in SILVACO ATLAS:

- Decoupled (GUMMEL)
- Fully coupled (NEWTON)
- BLOCK

The **GUMMEL** method solves for each unknown by keeping all other unknowns constant. The process is repeated until there is a stable solution. Newton's method solves all unknowns simultaneously. The **BLOCK** method solves some equations with the **GUMMEL** method and the others with the **NEWTON** method.

The **GUMMEL** method is used for a system of equations that are weakly coupled and where there is linear convergence. **NEWTON** method is used when the equations are strongly coupled with quadratic convergence. In our example, we used the following **Method** order

```
METHOD GUMMEL NEWTON BLOCK
```

In this example, equations are resolved by a GUMMEL method. If the convergence cannot be reached then NEWTON helped solve some of the equations and the others were solved by BLOCK.

4.4. Solutions Specification

So far, we have created the structure, allocated the materials to their specific regions, gave them their properties, specified the physical models, and selected the numerical method for the calculations to be done. The next step is to specify solutions.

To evaluate a solar cell created in DECKBUILD or any other structure defining program, the user can simulate the actual conditions in which a solar cell would operate. This includes variables such as a light beam with its associated optical intensity and angle of incidence, different voltage conditions on the electrodes, and temperatures, to then extract and study the important optical-electrical parameters such as:

- The Current-Voltage curve (I-V curve)
- The Short Circuit Current (I_{sc})
- The Open Circuit Voltage (V_{oc})
- The Fill Factor (FF)
- The Efficiency η (%)

4.4.1. Defining the light source

In simulating solar cells, the user must specify a **beam of light**, which shines upon the device, and can then use any number of electrode conditions and solve statements to gather the desired characteristics of our Graphene/GaAs solar cell.

In this work, the light beam and the electrodes are utilized to set the environment for obtaining solutions of solar cell simulations.

BEAM: In DECKBUILD, the `BEAM` statement, which is used in obtaining solar cell solutions, comes after all of the structure defining statements and before the following solve statements. The light beam defining statement in this work is the following:

```
Beam num=1 x.o=0.5 y.o=-0.5 angel=90 AM1.5
```

4.4.2. Obtaining solutions

Before inputting statements that obtain all of the pertinent solutions for a device, files must be created to store all of the following solutions. These files can be of two types: **.log** and **.str** (structure) files.

LOG:allows all final simulation characteristics to be saved in a .log file (saves a file of .log extension). Any type of data, whether I-V, transient or C-V, generated by the `SOLVE` command is saved after the `LOG` command (thus the saved information is of the electrical type and is, for example, dependent on the voltage Polarization or light source). If in the program there are several `LOG` commands, each time the log file that was opened before is closed, and a new log file is opened.

The following shows an example of the `LOG` statement.

```
LOG outfile=myoutputfile.log
```

The example saves the current-voltage information into `myoutputfile.log`, which can be viewed graphically in Tonyplot, which allows the user to specify the specific parts of the solution to a graph, as many solutions are all contained in one file and cannot be graphed simultaneously.

Structure files can be saved after a specific solve statement. This file stores all of the data from the solution and allows it to be viewed visually on the device structure. An example of the resulting structure file following a solve statement is given in Figure 23. Tonyplot can convert the numerical data saved into the structure file into a visual representation within the device.

After defining a log file in which all solutions are to be stored, ATLAS software does an initial solving of the doping profile and the potential at every mesh point in the zero-electrode bias case. This initial solution is obtained when there is no initial reference zero bias solution but can be specified by the statement `solve init`. After this initial solve statement, the conditions for the specific solve statements can be set. In simulating the operation of a solar cell.

SOLVE: The `SOLVE` statement follows the `LOG` statement. SOLVE performs a solution for one or more bias points. The following `SOLVE` statement is the one that was used in our study to obtain the solutions.

```
SOLVE b1=1.0
```

This statement applies the equivalent of **one sun** from the earlier defined light source (in `BEAM` statement) and solves the pertinent quantities, such as photogeneration rates and optical intensities, at each mesh point as well as the electrode currents.

After the beam of light has been applied, solutions at different electrode voltages can be obtained to create the solar cell's I-V curve.

```
solve vanode=0 name=anode vstep=0.1 vfinal=2.7
```

This statement is to obtain solutions for the illuminated solar cell at a range of anode voltages. It declares an initial anode voltage of 0 V and obtains solutions in the range from 0 V to 2.7 V in increments of 0.1 V.

By sweeping across anode voltages from 0 V to V_{oc} for the solar cell, the I-V curve is obtained. The results can later be displayed in Tonyplot in the form of a graph.

LOAD AND SAVE: The LOAD statement enters previous solutions from files as initial guess to other bias points. The SAVE statement enters all node point information into an output file.
The following are examples of LOAD and SAVE statements:

4.5. Results' Analysis

Once a solution has been found for a semiconductor device problem, the information can be displayed graphically with TonyPlot. Additionally, device parameters can be extracted with the `EXTRACT` statement, which can be written manually in DECKBUILD, or selected from the "Insert Extract" menu from the "Commands" button in DECKBUILD's menu bar.

In the example below, the `EXTRACT` statement obtains the current and voltage characteristics of a solar cell. This information is saved into the `IVcurve.dat` file,

then, TonyPlot displays the information in the IVcurve.dat file in the form of a graph.

```
EXTRACT NAME="iv" curve(v."anode", i."cathode") /
OUTFILE="IVcurve.dat"
TONYPLOT IVcurve.dat
```

The following figure is an example of a solar cell's I-V curve displayed in Tonyplot using a simulation script of a silicon solar cell, which came pre-installed with SILVACO (TCAD).

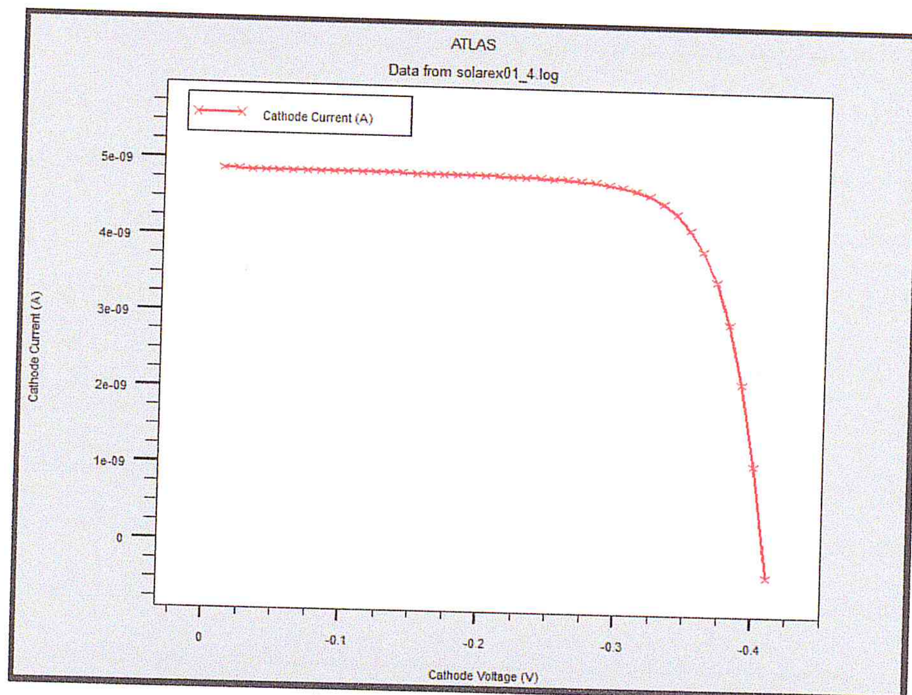

Figure 3-9. I-V curve of a silicon solar cell as it is displayed in Tonyplot

III.II. SIMULATION RESULTS AND DISCUSSION

1. INTRODUCTION

In this chapter, we are going to talk about the results that we have gathered from the simulation. The variations of i-layer thickness, are applied to observe their effect on the value of Efficiency, Fill Factor, V_{oc} and J_{sc}. The results are then compared with the results from article Ref.1. Therefore, we tried to replicate the one that was studied in article Ref.1.

The structure was obtained easily.

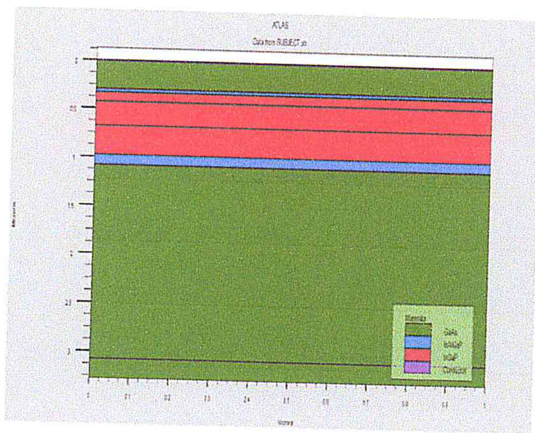

(a)

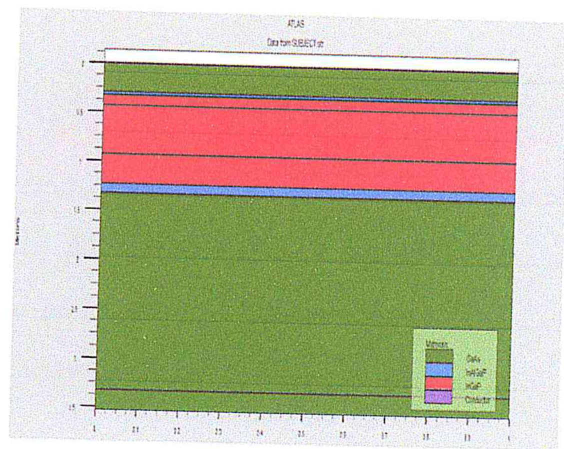

(b)

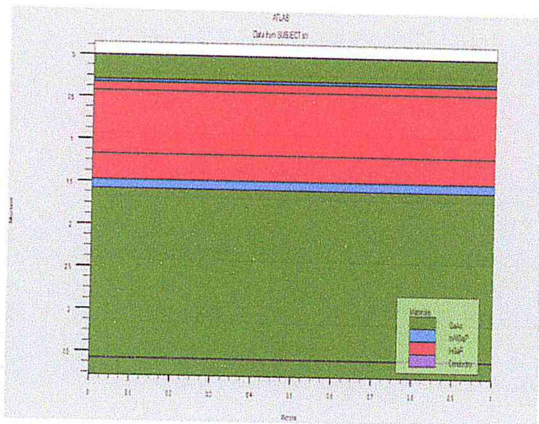

(c)

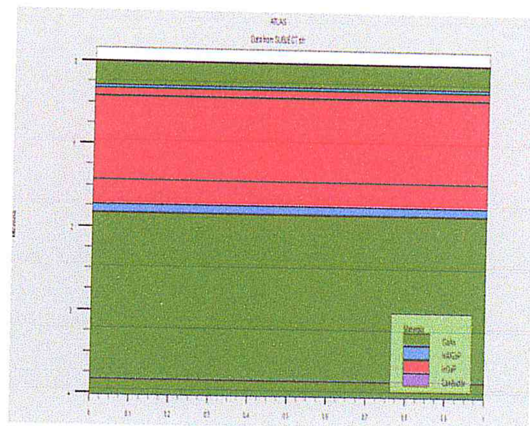

(d)

Figure 3-10: (a) (b) (c) and (d) are the struvtures obtained for different I-layer thicknesses.

2. RESULTS AND DISCUSSION

2.1. Evaluating Solar Cell's Electrical and Optical Properties

To evaluate the solar cell's performance, the thickness of the undoped GaInP substrate was varied. The different GaInP thicknesses that were used are: $0.25\mu m$, $0.5\mu m$, $075\mu m$ and $1\mu m$.

To obtain the electrical and optical characteristics of our solar cell, a sun illumination of 1.5 AM is simulated upon the structure of our solar cell. A forward bias current is then applied to its electrodes.

The important data, figures and graphs are stored into .log and .str files, then extracted and plotted using the "*extract*" command and "*Tonyplot*".

All obtained results of this work are summarized in the following table:

Table 3-1. Results of the simulation for different parameters.

Thickness µm	Workf	Doping	Jsc (mA/cm^2)	Voc (v)	FF	η (%)
0.25	3.5	None	4.5	1.36	74.93	3.36
0.5	3.5	None	4.5	1.32	76.13	3.32
0.75	3.5	None	4.5	1.29	78.18	3.32
1	3.5	None	4.5	1.28	78.45	3.66

The following figures represent the I-V curves of our GaInP p-i-n solar cell with the previous parameters of thicknesses:

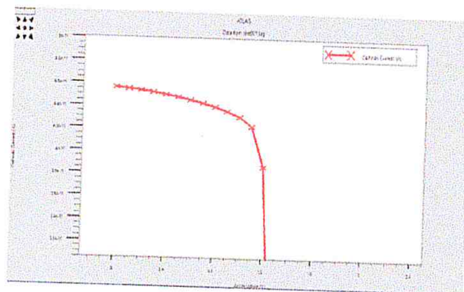

(a)

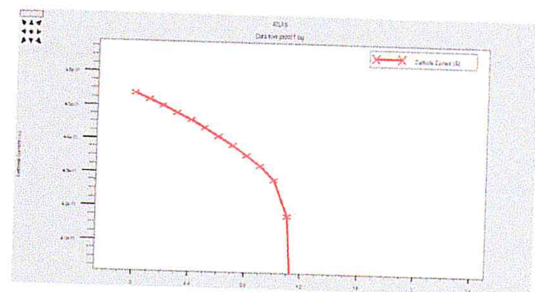

(b)

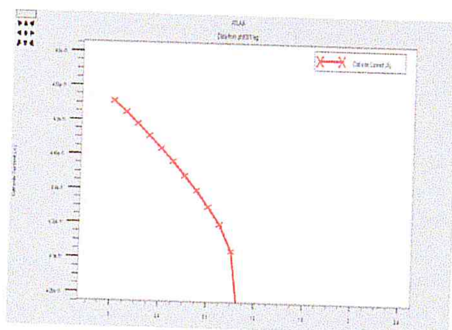

(b)

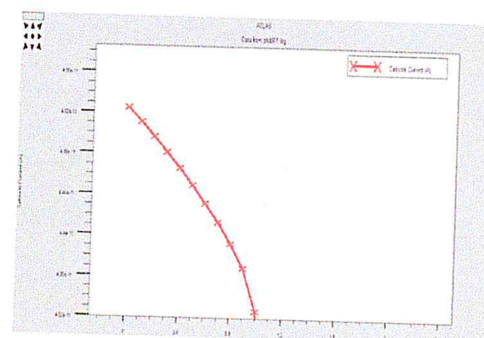

(d)

Figure 3-11: (a) (b) (c) and(d) represent th I-V curves of our InGaP P-I-N solar cell with different i-layer thicknesses.

3. CHAPTER SUMMARY

In this chapter, we have presented the software that was used in our work to simulate a GaInP P-I-N solar cell whith different I-layer thicknesses, seen what are the different steps to create the structure, allocate materials to it, give these materials their respective properties, study the optical-electrical behavior of our devices and extract the different results represented into graphs and numerical results.

These results showed us that the most optimized i-layer thickness is around (1μm)

Thus, we conclude that it is important to take these factors into consideration in future projects in this subject.

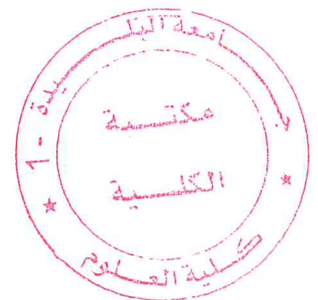

IIIV. General Conclusion

In coclusion, we have found approximately the same results as the paper[4] ,a series of expiriments determined the built-in electric field strengths and i-layer quality for all samples and confirmed that the optimized i-layer thickness is around (1μm) , for the sample with thinner i-layer thickness, solar cells could not absorb all of the sun light efficiently. Therefore, the short circuit current and output power would be low. In addition, a lot of point defects are generated inyhe samples with thinner i-layer and the built-in electric field is not high enough to drive out all of photo-induced current.

Solar cells are currently a high priority for both the military and the civilian sectors as a viable source of renewable energy, and as a power source in remote areas such as space or countryside. Research regarding the improvement in efficiency of solar cells have to be intensified in our universities and research centers, as nations are shifting from traditional sources of energy, such as fossil fuels, by attempting to generate more energy from renewable resources for domestic and industrial use, and to allow new technologies to be accessible in remote areas.

LIST OF SYMBOLS

Symbol	Name	Unit
h	Planck's constant	$eV.s$
ν	Photon frequency	s^{-1}
c	Light speed in vacuum	m/s
K_B	Boltzmann constant	$photons.cm^{-2}s^{-1}$
T	Room temperature	$°K$
q	Elementary charge	C
W	Depletion region width	μm
λ	Photon Wavelength	μm
N_C, N_V	Densities of State	cm^{-3}
E_F	Fermi energy state level	eV
E_C	Lowest level of energy in the conduction band	eV
E_V	Lowest level of energy in the valence band	eV
n_i	Intrinsic concentration	cm^{-3}
n	Density of free electrons	cm^{-3}
p	Density of free holes	cm^{-3}
ϕ_B	Schottky Barrier height	eV
ϕ_m	Metal work function	eV
χ	Electron affinity in a semiconductor	eV
V_{BI}	Built-in potential	eV
ϕ_s	Semiconductor work function	eV
N_a , N_d	Concentration of acceptors and donors respectively	cm^{-3}
V_{OC}	Open circuit voltage	V
V_A	Applied voltage	V
V_{max}	Maximum power voltage	V
I_{SC}	Short circuit current	mA
I_F	Forward bias current	mA
I_{max}	Maximum power current	mA
I_0	Initial current	mA
I_R	Reverse bias current	mA
k	Boltzmann's constant	$eV.K^{-1}$
A	Area of contact between metal and semiconductor	cm^2
R_S	Series resistance	Ω
V_{RB}	Reverse Bias Voltage	V
ε_m	Permittivity in metal	$\mathrm{F \cdot cm^{-1}}$
ε_0	Permittivity in vacuum	$\mathrm{F \cdot cm^{-1}}$
P_{max}	Maximum power	$Watts$
FF	Fill Factor	%
η	Efficiency	%
$A.M$	Air mass	
E	Photon energy	eV
E_g	Energy Bandgap	eV
$GaAs$	Gallium Arsenide	
Si	Silicon	
$4H-SiC$	Silicon carbide	

τ_c	Mean free time between collisions	s
$\underline{n}$	Complex refractive index	
n	Real part of the complex refractive index	
κ	Imaginary part of the complex refractive index	
R_{SH}	Sheet resistance	Ω/sq
ρ	Resistivity	$\Omega.cm$
μ_n, μ_p	Electron and hole mobilities	$cm^2/V.s$

[25] Reference Solar Spectral Irradiance & PV Cell Operational Regions (ASTM G173-03) ASTM

.

[28] III-V compound semiconductor material systems *"Design, fabrication, characterization and modeling of: High Electron Mobility Transistors, RTD, Gunn diodes, nanocolumns."* ISG-1, Research Center Juelich, Germany.

[138] Atlas User's Manual*"Device Simulation Software"*, Silvaco, Inc.4701 Patrick Henry Drive, Bldg. 2. Santa Clara, CA 95054 (2016).